

On the relationship between the periodic and aperiodic variability of accreting X-ray pulsars

Davide Lazzati

Osservatorio Astronomico di Brera
Via E. Bianchi, 46 – 22055 Merate (Lecco), Italy

and

Università degli Studi di Milano - sede di Como
Via Lucini, 3 – 22100 Como, Italy
E-mail: lazzati@merate.mi.astro.it

Luigi Stella¹

Osservatorio Astronomico di Roma
Via dell'Osservatorio, 2 – 00040 Monteporzio Catone (Roma), Italy
E-mail: stella@coma.mporzio.astro.it

¹ Affiliated to the International Center for Relativistic Astrophysics

ABSTRACT

Besides the narrow peaks originating from the periodic signal, the power spectra of accreting X-ray pulsars display continuum components usually increasing towards low frequencies; these arise from the source aperiodic variability. Most studies so far adopted the view that the periodic and aperiodic variations are independent. However any aperiodic variability in the emission from the accretion column(s) towards the magnetic neutron star should be modulated at the X-ray pulsar period, by virtue of the same rotation-induced geometric effects which give rise to the periodic signal. We develop here a simple shot noise model to test the presence of a coupling between the periodic and aperiodic variability of X-ray pulsars. The model power spectrum is fit to the power spectra of three X-ray pulsars, Vela X-1, 4U 1145-62 and Cen X-3 observed with EXOSAT. In the first two cases we find that a highly significant coupling is present, as testified by a substantial broadening in the wings of the power spectrum peaks due to the periodic modulation. We find also that these wings can mimic the presence of a knee in the continuum power spectrum components around the fundamental of the periodic modulation, therefore questioning the correlation reported by Takeshima (1992) between the X-ray pulsar frequency and the knee frequency, beyond which the continuum power spectral component steepens.

Subject headings: X-rays: binaries — Pulsars — Stars: accretion — Stars: neutron — Stars: X-rays

1. Introduction

That fast aperiodic X-ray flux variations are present in accreting magnetic neutron stars became clear with the discovery of 4.4 s pulsations from V0332+53, a transient X-ray binary that had tentatively been classified as a black hole candidate based on the similarity of its short term variability to that of Cyg X-1 (Tanaka et al. 1983, Stella et al. 1985, Makishima et al. 1990). A number of studies of the aperiodic variations of X-ray pulsars has been carried out since. In most cases these studies have relied upon power spectrum techniques in a way that parallels the application to non-pulsating X-ray binaries. Continuum power spectrum components arising from the source aperiodic variability are often identified, fit to analytic models and used to characterise the short term variations in relation to other source properties (such as spectral or luminosity state). These continuum power spectrum components provide also an important element for classifications across different types of accreting X-ray sources (see e.g. van der Klis 1995 and references therein).

In addition to the narrow peaks originating from the periodic modulation, the power spectra of many X-ray pulsars show distinct noise component(s) increasing towards low frequencies. In several of the slower wind-fed X-ray pulsars the power increases in a power law-like fashion down to the lowest frequencies sampled (usually $10^{-4} - 10^{-3}$ Hz). Some of the faster disk-fed X-ray pulsars show instead a (nearly) flat-topped noise component at low frequencies which steepens above a knee at a frequency of ν_{knee} (Nagase 1989; Soong and Swank 1989). To date the most detailed and comprehensive study of the power spectra of X-ray pulsars has been carried out by Takeshima (1992), based on Ginga observations. This author reports that a flat-topped or a moderately steep noise component is present in virtually all X-ray pulsars shortwards of the peak corresponding to the fundamental of the periodic modulation. In many cases the knee above which the power spectrum steepens lies close to the base of this peak, such that a strong correlation is found between the pulse frequency ν_p and the knee frequency ν_{knee} , centered around the relation $\nu_s \simeq \nu_{knee}$ (Takeshima 1992).

Several other continuum power spectrum features extending over a more limited range of frequencies (usually a decade or less) are observed in X-ray pulsars: these include broad bumps, wiggles and steep very low frequency excesses. Broad power spectrum peaks

testifying to the presence of quasi periodic oscillations have been clearly revealed in some cases, notably Cen X-3 (Nagase 1989; Soong and Swank 1989), EXO 2030+375 (Angelini et al. 1989), 4U 1626-67 (Shinoda et al. 1990) and A0535+262 (Finger et al. 1996). The continuum power spectrum components of individual X-ray pulsars have been observed to change in relation to a variety of phenomena such as source flux, orbital phase and spin-up versus spin-down (Angelini 1989; Angelini et al. 1989; Belloni & Hasinger 1990a; Parmar et al. 1989).

Most studies so far implicitly adopted the view that the periodic and aperiodic variability of X-ray pulsars are independent, such that the light curves are given by the sum of the two corresponding signals; similarly the power spectra are given by the sum of the individual power spectra of the two signals (see e.g. Angelini et al. 1989). On the other hand it is well known that X-ray pulsars generate their periodic signal by virtue of geometric effects arising from the rotation-induced motion of the accretion column(s) through which the inflowing material is funneled onto the magnetic poles of the neutron star. Any aperiodic variation in the emissivity of the accretion column(s) should therefore be modulated by the periodic signal as well. Accordingly, Makishima (1988) suggested an approach in which the aperiodic variability of an X-ray pulsar is multiplied by (as opposed to summed to) the periodic modulation. The coupling between the aperiodic and periodic variations, if present, is expected to alter the shape of the power spectrum, due to the convolution of the corresponding Fourier transforms (see also Burderi et al. 1993).

In this work, we develop a simple model for testing the presence of a coupling between the aperiodic variability of X-ray pulsars and their periodic signal. We adopt a suitable shot noise model to work out analytically the expected power spectrum for an arbitrary coupling factor. The model power spectrum obtained in this way is then fit to the power spectra of several X-ray pulsars. In two out of three cases we find that a significant coupling is present between the shots and the periodic signal, as testified by a substantial broadening in the wings of the power spectrum peaks arising from the periodic modulation. In these two cases the continuum power still increases shortwards of the periodic modulation peak(s) and the broad wings mimic the presence of a knee in the power continuum close to ν_p . By analogy this suggests that also in other X-ray pulsars with extended red noise components the power spectrum knee close to $\sim \nu_p$ might be an artifact produced by the broad wings of the coherent modulation peak(s); therefore, the reported correlation between ν_p and ν_{knee} appears to be questionable.

Our paper is organised as follows: Section 2 describes the analytic shot noise model that we have developed; the application of this model to the power spectra from the EXOSAT light curves of selected X-ray pulsars is described in Section 3; our results are

discussed in Section 4.

2. The shot noise model

Shot noise models provide a useful mathematical description of the accretion flow inhomogeneities that are believed to generate the variability of accreting compact stars (Terrell 1972; Weisskopf et al. 1975; Sutherland et al. 1978; Shibazaki & Lamb 1987; Elsner et al. 1987; Abramowicz et al. 1991). Individual shots are often supposed to be representative of the emission from self-luminous blobs or clumps in the accretion process. In the context of accreting X-ray pulsars, models involving density fluctuations in the accreting plasma have been discussed by Burderi et al. (1993) and Hoshino & Takeshima (1993).

We assume that the X-ray pulsar signal consists of two different components: (1) a deterministic periodic component:

$$f_1(t) = A + \sum_{n=1}^N B_n \sin(n\omega_0 t + \phi_n) \quad ,$$

where $\omega_0 = 2\pi/P$ is the fundamental of the pulsed signal of period P , N the number of its harmonics and ϕ_n the corresponding phases; (2) an aperiodic component consisting of the superposition of a number of similar shots, which gives rise to the red noise power spectra observed in most X-ray pulsars. In order to reproduce the complex characteristics of the red spectra which are frequently observed (such as, e.g., different power law slopes in different frequency ranges) most authors adopt a simple (usually exponential) shot shape, and consider suitable distributions of shot amplitudes and decay times (see e.g. Belloni and Hasinger 1990b and references therein). We adopt a somewhat complementary model in which all shots have the same shape and amplitude (described by the envelope function $g(t)$), such that their superposition is given by

$$\tilde{f}_2(t) = \sum_j g(t - t_j) \quad ,$$

where t_j is the (random) start time of the j^{th} shot. This model is more easily handled analytically and yet yields model power spectra of arbitrary complexity.

If the aperiodic component is coupled to the periodic one, then f_2 is, at least in part, modulated by f_1 . Therefore we write

$$f_2(t) = \left[1 + \frac{C'}{A} \sum_{n=1}^N B_n \sin(n\omega_0 t + \phi_n) \right] \tilde{f}_2(t) \quad ,$$

with C' a constant that controls the extent to which the periodic signal modulates the shots (the lower C' , the lower the modulation). In order to leave the fluence of each shot unaffected (at least on average), we have divided the amplitude of the deterministic function by its mean value A . Note that A cannot be derived directly from the mean value of the signal, since this comprises an additional term given by the mean of the shots. Therefore we define a new constant, $C = C'/A$, which controls the degree of modulation but is inversely proportional to the mean signal. The CB_i products provide a measurement of the depth of the shot modulation in each harmonics.

The Fourier transform of the X-ray pulsar signal $f_\infty(t) = f_1(t) + f_2(t)$ is therefore

$$\begin{aligned} F_\infty(\omega) = & A\delta(\omega) + \sum_{n=1}^N \frac{B_n}{2i} e^{-i\omega\phi_n} [\delta(\omega - n\omega_0) - \delta(\omega + n\omega_0)] + \\ & + \left\{ \delta(\omega) + \frac{C}{2i} \sum_{n=1}^N B_n e^{-i\omega\phi_n} [\delta(\omega - n\omega_0) - \delta(\omega + n\omega_0)] \right\} * \left\{ G(\omega) \sum_j e^{-i\omega t_j} \right\} \quad , \end{aligned}$$

where $G(\omega)$ is the Fourier transform of the shot envelope function $g(t)$.

For practical applications, the power spectrum must be calculated by taking into account the effects due to the binning, sampling and finite duration of the light curves. Following van der Klis (1989) we describe a finite, equispaced and binned light curve as (“*” indicates a convolution)

$$f(t) = \{ [f_\infty(t)w(t)] * b(t) \} s(t) \quad , \quad (1)$$

where $b(t)$ is the binning function, $s(t)$ the sampling function (a monodimensional lattice) and $w(t)$ the window function. By using the convolution theorem, the Fourier transform $F(\omega)$ of $f(t)$ writes

$$F(\omega) = 2\pi \{ [F_\infty(\omega) * W(\omega)] B(\omega) \} * S(\omega) \quad , \quad (2)$$

where the Fourier transforms of $w(t)$ and $b(t)$ are, respectively,

$$\begin{aligned} W(\omega) &= \frac{T}{2\pi} \text{sinc}\left(\frac{T}{2}\omega\right) \sim \delta(\omega) \\ B(\omega) &= \frac{\Delta t}{2\pi} \text{sinc}\left(\frac{\Delta t}{2}\omega\right) \quad , \end{aligned}$$

where $\text{sinc}(x) = \frac{\sin(x)}{x}$. $S(\omega)$ is the reciprocal lattice. T and Δt indicate, respectively, the light curve duration and its binning time. Note that in Eq. 2 we have used the normalisation

$$F(\omega) = \frac{1}{2\pi} \int_{\mathbf{R}} f(t) e^{-i\omega t} dt \quad .$$

The convolution with $S(\omega)$ in Eq. 2 can be neglected, as the aliasing introduced by the sampling is depressed by the sinc due to the binning. Moreover the observed power spectra (see Section 3) are often dominated by the counting statistics noise well before the Nyquist frequency, such that the low signal to noise further reduces the possibility of detecting any alias. The expression for $F_\infty(\omega)$ in Eq. 2 can be simplified by neglecting the δ -functions centered on negative frequencies. Therefore for $F(\omega)$ we obtain

$$\begin{aligned} F(\omega) &= \frac{\Delta t}{2\pi} \text{sinc}\left(\frac{\Delta t}{2}\omega\right) \left\{ AT \text{sinc}\left(\frac{T}{2}\omega\right) + \frac{T}{2i} \sum_{n=1}^N B_n e^{-in\omega_0\phi_n} \text{sinc}\left[\frac{T}{2}(\omega - n\omega_0)\right] + \right. \\ &\quad \left. + 2\pi \left\{ G(\omega) \sum_j e^{-i\omega t_j} + \frac{C}{2i} \sum_{n=1}^N \left[B_n e^{-in\omega_0\phi_n} G(\omega - n\omega_0) \sum_j e^{-i(\omega - n\omega_0)t_j} \right] \right\} \right\} \quad , \quad (3) \end{aligned}$$

where $W(\omega)$ was approximated with a δ -function in the convolution with G , since the shot decay time is supposed to be much shorter than the observation duration T (such that $G(\omega)$ is much wider than $W(\omega)$).

The final step is to calculate the power spectrum $P(\omega)$. As usual, the simple definition $P(\omega) = |F(\omega)|^2$ cannot be adopted as it would include a strong dependence on the shot start times. Instead the definition

$$P(\omega) = \langle |F(\omega)|^2 \rangle \quad (4)$$

must be used, where the brackets indicate the average over the ensemble of realisations of signals with the same deterministic periodic component and shot parameters, but with different $\{t_j\}$. The derivation of $P(\omega)$ is quite complex, and is described in the Appendix. The result is

$$\begin{aligned}
 \text{(a)} \quad P(\omega) &\simeq \frac{\Delta t^2}{4\pi^2} \text{sinc}^2\left(\frac{\Delta t}{2}\omega\right) \left\{ T^2(A + \bar{E})^2 \text{sinc}^2\left(\frac{T}{2}\omega\right) + \right. \\
 \text{(b)} \quad &+ \frac{T^2}{4} \sum_{n=1}^N B_n^2 \text{sinc}^2\left[\frac{T}{2}(\omega - n\omega_0)\right] + \\
 \text{(c)} \quad &+ 4\pi^2 T\nu \left[|G(\omega)|^2 + \frac{C^2}{4} \sum_{n=1}^N B_n^2 |G(\omega - n\omega_0)|^2 \right] + \\
 \text{(d)} \quad &+ C^2 \pi^2 (T^2 \nu^2 - T\nu) \sum_{n=1}^N B_n^2 |G(\omega - n\omega_0)|^2 \text{sinc}^2\left[\frac{T}{2}(\omega - n\omega_0)T\right] + \\
 \text{(e)} \quad &+ 2\pi^2 T^2 \nu C \sum_{n=1}^N B_n^2 |G(\omega - n\omega_0)|^2 \text{sinc}^2\left[\frac{T}{2}(\omega - n\omega_0)T\right] \left. \right\} , \tag{5}
 \end{aligned}$$

where ν is the shot rate, and \bar{E} the mean power in the shot component. It is worth emphasising that the formula above is derived under the assumption that the observation duration T is long enough that the cross-terms resulting from the relative phases in the harmonics of the periodic signal can be neglected (see the Appendix). The validity of this assumption is verified *a posteriori* in the application to the observed power spectra of selected X-ray pulsars presented in Section 3.

Besides the multiplicative term due to the binning, the right hand side of Eq. 5 comprises four additive terms; these are, respectively:

(a) The term arising from the average level of the total signal, i.e. the deterministic periodic signal plus the shot noise. This term is sharply peaked around zero frequency.

(b) The term containing the narrow peaks (width of $\sim 1/T$) due to the N harmonics of the deterministic periodic signal.

(c) A term consisting of the sum of the red noise spectrum due to the shots' envelope ($|G(\omega)|^2$) plus broad wings (width of $\sim \frac{1}{\tau}$, where τ is the characteristic decay-time of the shots) centered around each narrow peak. These broad wings are characterised by the same functional form of the red noise spectrum on both sides of each peak. They arise from the convolution of the deterministic signal peaks with the red noise component due to the shots.

(d) An additional term contributing to the narrow peaks (width of $\sim 1/T$) centered around the harmonics. This term is due to the fact that the modulation of all shots is in phase with respect to the deterministic periodic signal. In principle this contribution to the narrow peaks could be distinguished from that due to the deterministic narrow peaks (term *b*) by virtue of the dependence on the shot rate ν .

(e) A term, contributing to the narrow peaks' amplitude, which arises from the cross product in the calculation of the squared modulus of the two terms in Eq. 3. Its amplitude is a factor of $\sim C\nu$ lower than term *d*.

Within our model the presence of broad wings around the peaks (see term c) unambiguously indicates that the shots are modulated by the periodic signal, such that a coupling is present. Note that the functional form of the broad wings is dictated by the red noise component, such that the modelling of the wings (that usually have a poor signal to noise ratio) is coupled to the modelling of the red noise component. It should be emphasized that no assumption is yet made about envelope function of the shots.

The possibility of revealing a modulation of the shots through the broad wings of the narrow peaks depends crucially on the ratio of the pulsar period to the characteristic decay time τ of the shots. To illustrate this point we show in Fig. 1 the model power spectra obtained for shots with exponential envelope function and decay-time $\tau = 300$ s. The different curves correspond to 50% modulated shots with a sinusoidal signal of period $P = 236, 471, 942, 1885, 3770$ s, respectively. It is apparent that when $2\pi P \gtrsim \tau$ the wings are so broad that they become virtually indistinguishable from the red noise. This is due to the fact that the shots are too short-lived to display a conspicuous periodic modulation.

3. Application to the Power Spectra of selected X-ray Pulsars

3.1. Fitting procedure

In order to test the coupling between the periodic and aperiodic variability, we used the model power spectrum in Eq. 5 to fit the power spectra obtained from the X-ray light curves of a few selected X-ray pulsars. The relevant formula was inserted in the QDP/PLT fitting program (Tennant 1981), which provides a nonlinear least square fitting based on the Marquandt method. A constant term was added to account for the presence of counting statistics (white) noise in the power spectra.

We used the [4–9] keV light curves of X-ray pulsars obtained with the EXOSAT Medium Energy detector array, in consideration of their high statistical quality and (near) absence of interruptions (White and Peacock 1988). The data were extracted from the High Energy Astrophysics Database System at the Brera Astronomical Observatory (Tagliaferri & Stella 1993, 1994, see also White et al. 1995a). For each source a power spectrum was calculated over a number of separate observation intervals of the same length. For each interval we checked that: (a) the source count rate was approximately at the same level; (b) the light curves did not contain eclipses, absorption dips or other non-stationary events; (c) the position of the narrow peaks due to the periodic pulsar signal was the same to within the Fourier resolution $1/T$ of the power spectra (such that the smearing due to the orbital Doppler effect and secular period derivative could be neglected).

As customary, we calculated the power spectra of each interval after subtracting the average count rate, such that the contribution of term a in Eq. 5 can be neglected and the term itself excluded from the fit. These power spectra were then used to produce an average power spectrum for each X-ray pulsar. The statistical error of the power estimates was evaluated based on the standard deviation of the average power for each Fourier frequency. Note that the interval duration was determined by compromising between two conflicting requirements: that the intervals are long enough to investigate the low frequency end of the red-noise and that their number is high enough (we averaged a number of 7 to 13 individual spectra) to make the distribution of the power estimates in the average power spectrum close to a Gaussian distribution (as required to apply standard least square fitting techniques, see e.g. Israel & Stella 1996 and references therein).

In the EXOSAT database we identified three X-ray pulsars, with observations meeting the above requirements. These are Vela X-1 ($P = 282.6$ s), 4U1145-62 ($P = 292.1$ s) and Cen X-3 ($P = 4.8$ s) (see e.g. Nagase 1989; White et al. 1995b and references therein). Details of the relevant observations are given in Table 1, together with the interval length and binning time adopted in our analysis.

The fitting procedure for the average power spectrum of each X-ray pulsar consists of three steps.

(i) First we fit our model under the hypothesis that no coupling is present between the deterministic periodic signal and the shots. This is obtained by setting $C = 0$. Consequently terms d and e and the 2nd part of term c of Eq. 5 are excluded from the fit. Therefore this case includes only the red noise component and the “narrow peaks” (under the assumption that the effects of the relative phases between the harmonics can be neglected). For $|G(\omega)|^2$ we find that a King-like model of the form

$$|G(\omega)|^2 = D \left[1 + \left(\frac{\omega}{\omega_c} \right)^2 \right]^{-\alpha} \quad (6)$$

reproduced quite accurately the power law-like behaviour and the low frequency flattening that characterizes the red noise spectra we analysed.

(ii) The model used in step (i) is generalised to include the effects due to the relative phases between the harmonics. The relevant formula is given by Eq. 11 in Angelini et al. (1989). This step is designed to provide an *a posteriori* check of the assumptions under which Eq. 5 has been derived.

(iii) In the third step the model that includes the coupling between the periodic signal and the red noise is used. In this case the coupling constant C of Eq. 5 is used as a free

parameter in the fit. The only contribution to the broad peak wings derives from the second part of term c in Eq. 5. Note that the shape of the broad wings depends on $|G(\omega)|^2$, which in turn is mainly determined by the shape of the red noise. In practical applications of Eq. 5, it is found that the signal to noise of the observed power spectra is insufficient to isolate the contribution to the narrow peaks deriving also from terms d and e of Eq. 5. Therefore we carry out the fit by neglecting these two terms. In this approach the shot rate cannot be obtained directly from the fit to the power spectrum. Moreover the value of C , which is related to the ratio between the height of the narrow peak and broad wing component, is underestimated. This is because, by neglecting terms d and e in Eq. 5, the height of the narrow peaks is attributed only to the deterministic component. A value of C significantly different from zero would nevertheless reveal the presence of a coupling.

3.2. Vela X-1

The average power spectrum of Vela X-1 obtained from the 4-9 keV EXOSAT light curves is shown in Fig. 2. The fit obtained under the hypothesis of no coupling (step i) is shown in the upper panel of Fig. 2, while the corresponding residuals are shown in the lower panel. The fit to the red noise provides a King model index of $\alpha \simeq 0.58$, whereas the break frequency $\nu_c = \omega_c/2\pi$ was too low to be measured. The fit included the first eleven harmonics of the pulse frequency $\nu_p = (3.5379 \pm 0.0007) \times 10^{-3}$ Hz. The corresponding χ^2 is 325.9 for 189 degrees of freedom (hereafter dof). It is apparent that the peak wings are not well modelled. Including the effects of the relative phases between the harmonics (step ii) left the best fit and corresponding χ^2 (=323.3) virtually unaffected, while the number of dof decreased to 180. An F-test for the addition of 9 free parameters, confirmed that the improvement of the fit is not significant.

Having checked that the relative phases between the harmonics can be neglected, we proceeded to step iii by allowing for a periodic modulation of the shots (the coupling constant C is now treated as a free parameter). A much better fit is obtained in this case with $\chi^2/dof = 229.3/188$. This corresponds to an F-test chance probability of $< 10^{-15}$ for the addition of one free parameter with respect to the fit of step i . Fig. 2(b) shows that the new fit reproduces far more accurately the broad wings of the peaks. For the red noise component, the new fit provides a break frequency of $\nu_c = (2.0 \pm 1.3) \times 10^{-4} Hz \ll \nu_p$ and a King model index of $\alpha = 0.72 \pm 0.05$ (errors are 90% confidence). The products CB_n of the coupling constant and the harmonics' amplitude obtained from the fit are given in Table 2.

It is useful to define a parameter $R = C \sum_{n=1}^N B_n$ which is related to the degree of

modulation of the pulse. In the case of a sinusoidal signal, R represents the relative depth of the periodic modulation of the shots. For a periodic signal containing more than one harmonics, the shape of the shot modulation cannot be reconstructed due to the absence of information about the relative phases of the harmonics. Consequently in this case R does not measure the relative modulation of the shots and values of $R > 1$ can be obtained. Nevertheless the value of R provides an indication of whether the shots are weakly ($R \ll 1$) or strongly ($R \approx 1$) modulated. For Vela X-1 we find a large value of $R = 3.2 \pm 0.2$, pointing to a large amplitude of the shot modulation.

3.3. 4U1145-62

The average power spectrum of 4U1145-62 was obtained from the X-ray light curves of separate EXOSAT observations, since no single long observation was available (cf. Table 1). The fit obtained under the hypothesis of no coupling between the periodic and the red noise (step *i*) is shown in the upper panel of Fig. 3(a). The first five harmonics of the pulsar modulation at $\nu_p = (3.4229 \pm 0.0006) \times 10^{-3}$ Hz were included in the fit. Note that in this case the red-noise component extends in a power law fashion down to the lowest frequencies sampled in the power spectrum ($\alpha = 0.41 \pm 0.02$), such that only an upper limit to the break frequency $\nu_c \lesssim 10^{-4}$ Hz could be obtained. This frequency is $\ll \nu_p$, like in the case of Vela X-1. For step *i* and step *ii* fits a χ^2 of 299 was obtained, respectively for 189 and 180 *dof*. Therefore also in this case the effects of the relative phases between the harmonics are negligible. When the coupling constant C was allowed to vary (step *iii*) we find a χ^2/dof of 275/188; correspondingly the F-test chance probability for the addition of one free parameter relative to the step *i* fit was found to be $\sim 3 \times 10^{-5}$. Therefore we conclude that also in the case of 4U1145-62 the shots are modulated. The values of CB_n are given in Table 2, while for R we derive a value of 1.6 ± 0.2 .

3.4. Cen X-3

The power spectrum of the EXOSAT light curves of Cen X-3 is different from the two cases presented above in that the red noise component shows a clear flattening for frequencies shorter than the fundamental of the periodic modulation (see Fig. 4), implying that the shot duration is comparable to the X-ray pulsar period. Under these circumstances, any modulation of the shots with the periodic signal would give rise to such broad wings around the power spectrum peaks, that they would be hardly distinguishable from the red noise itself (see Section 2). We confined our analysis of the power spectrum of Cen X-3 to

the range of frequencies between 0.02 and 0.8 Hz, such that the King-like model of Eq. 6 provided a reasonably accurate fit of the red-noise component. The first three harmonics of the periodic modulation at $\nu_p = (2.0692 \pm 0.0008) \times 10^{-1}$ Hz were included in the fit.

Under the hypothesis of no coupling, the fit (step *i*) gives a χ^2/dof of 2108/1589, for $\alpha = 0.43 \pm 0.03$ and $\nu_c = 1.2 \pm 0.1$ Hz. The step *ii* fit produced the same χ^2 , for 1580 *dof*; the effects of the relative phases between harmonics are therefore negligible also in the case of Cen X-3. Allowing for a periodic modulation of the shots (step *iii*) yielded a fit with a χ^2 of 2108, for 1588 *dof*. This shows that no broad wings are detected around the peaks in the case of Cen X-3 (see Table 2 for upper limits on the CB_n). Note however that since the expected shape of the wings is dictated by the shape of the red-noise (see above), only a poor upper limit is found for R ($\lesssim 0.66$ at the 90% confidence level). This indicates that a fairly strong coupling between the periodic and aperiodic variability might be present and remain undetected in Cen X-3.

4. Discussion

Based on a simple model consisting of the sum of a periodic signal plus random shots characterised by an arbitrary degree of modulation with the periodic signal, we have shown that in two out of three X-ray pulsars that we have analysed (Vela X-1 and 4U1145-62) there exists a strong coupling between the periodic and red noise variability. This coupling is revealed through the broad wings that are found around the power spectrum peaks arising from the periodic X-ray pulsar signal. As the shape of the red noise component dictates the shape of the broad wings, these are more easily detected when the red noise power increases shortwards of the pulsar frequency ν_p . This is indeed the case for Vela X-1 and 4U1145-62. On the contrary, the red noise component of Cen X-3 flattens around ν_p , such that any wings would be so broad that they are very difficult to separate from the red-noise component. We find no evidence for such very broad wings around the power spectrum peaks of Cen X-3; the corresponding upper limit to the modulation of the shots is poor and still allows for a relatively strong coupling. This is likely the case also in other disk-fed X-ray pulsars that show unambiguously a flat-topped red noise component steepening above frequencies of $\gtrsim \nu_p$.

Our results therefore suggest that a coupling between the periodic and red noise variability might be frequently present in X-ray pulsars. This is not a surprising result as one would expect that any accretion flow inhomogeneity (or “shot”) responsible for the red noise, produces most of its X-ray luminosity in the accretion column close to the neutron star surface. The combination of rotation and radiative transfer effects should

therefore produce a periodic modulation of the shots similar to that of any continuum X-ray accretion onto the polar caps. If, as assumed in our model, the modulation across different shots is phase coherent, then narrow power spectrum peaks are also generated by the shot component (see Section 2). One might speculate that the whole X-ray flux is produced by the superposition of random modulated shots (*i.e.* no deterministic periodic signal is present). To ascertain whether this is the case is beyond the scope of the present paper.

There is also an interesting consequence of our work concerning the correlation between the pulsar frequency and the knee frequency in the power spectrum continuum that was reported by Takeshima (1992). It is apparent from the power spectrum of Vela X-1 in Fig. 2 that the broad wings around the peaks might mimic the presence of a break in the red noise component around ν_p . To address this point in a quantitative fashion we adopted the power spectrum model used by Takeshima (1992). This comprises the sum of: (a) the narrow peaks from the periodic component; (b) a power law; (c) a flat component followed by a power law above a knee frequency ν_{knee} . The fit to the power spectrum of Vela X-1 obtained in this way is given in the upper panel of Fig. 5, showing also the separate contributions from the three model components. A value of χ^2/dof of 297/186 was obtained; this is considerably worse than the fit based on our modulated shot noise model ($\chi^2/dof = 229/188$). The bottom panel of Fig. 5 shows also the latter fit, with the separate contributions from the red noise, the narrow peaks and the broad wings. It is apparent that the broad wings provide a much more accurate fit of the power spectrum in between the narrow peaks. We conclude that the red noise power spectrum of Vela X-1 shows no evidence of a knee around ν_p . A similar conclusion, though with a lower statistical significance, is reached also for the power spectrum of 4U 1145-62. In this case we obtained a χ^2/dof of 299/189, 284/186 and 272/188 for the step (i) fit, the Takeshima model and the step (iii) fit, respectively.

By analogy, this suggests that also for other X-ray pulsars with red noise components increasing shortwards of ν_p , the broad wings resulting from the modulated shots might mimick the additional component with a knee at $\nu_{knee} \sim \nu_p$ that was introduced by Takeshima (1992). Therefore this component is probably not required and a red noise knee, if present, would be at $\nu_{knee} \ll \nu_p$. On the other hand, the case of Cen X-3 is probably typical of those X-ray pulsars for which the red noise flattens indeed below frequencies of $\nu_{knee} \gtrsim \nu_p$; any broad wings would be (nearly) undetectable and their contaminating effect on the power spectrum continuum negligible. The discussion above indicates that, if the power spectrum model does not include the broad wings around the periodic modulations peaks, a bias towards the $\nu_{knee} \sim \nu_p$ relation is likely introduced.

This is but an example of the caution that should be used in isolating the continuum

power spectrum components that arise *only* from the aperiodic variability of X-ray pulsars. Indeed the peaks' broad wings originating from the coupling of the periodic and aperiodic variability, if not adequately modelled, can lead to inaccurate conclusions concerning the shape, amplitude and frequency range of the continuum power spectrum components. A systematic reanalysis of the Ginga power spectra of X-ray pulsars should be carried out in the light of our present work. Valuable new information should derive from the X-ray pulsar power spectra that are being obtained by the RXTE.

LS acknowledges useful discussions with L. Angelini. This work was partially supported through ASI grants.

A. Appendix

The derivation of Eq. 5 begins with the application of definition 4 to Eq. 3. By averaging over the ensemble of different realisations of the shots start times $\{t_j\}$, we obtain:

$$P(\omega) = \frac{\Delta t^2}{4\pi^2} \text{sinc}^2\left(\frac{\Delta t}{2}\omega\right) \left\langle \left| AT \text{sinc}\left(\frac{T}{2}\omega\right) + \frac{T}{2i} \sum_{n=1}^N B_n e^{-in\omega_0\phi_n} \text{sinc}\left[\frac{T}{2}(\omega - n\omega_0)\right] + 2\pi \left\{ G(\omega) \sum_j e^{-i\omega t_j} + \frac{C}{2i} \sum_{n=1}^N \left[B_n e^{-in\omega_0\phi_n} G(\omega - n\omega_0) \sum_j e^{-i(\omega - n\omega_0)t_j} \right] \right\} \right|^2 \right\rangle .$$

As $T\omega_0$ is $\gg 1$, the interference terms between different harmonics can be neglected. In this limit the sinc function is approximated by a δ -function. A consequence of this is that also the relative phases between the harmonics are neglected. As described in Section 3, this assumption is verified *a posteriori* in the fitting procedure. We therefore obtain:

$$\begin{aligned} \text{(a)} \quad & P(\omega) = \frac{\Delta t^2}{4\pi^2} \text{sinc}^2\left(\frac{\Delta t}{2}\omega\right) \left\{ A^2 T^2 \text{sinc}^2\left(\frac{T}{2}\omega\right) + \frac{T^2}{4} \sum_{n=1}^N B_n^2 \text{sinc}^2\left[\frac{T}{2}(\omega - n\omega_0)\right] + \right. \\ \text{(b)} \quad & \left. + 4\pi^2 \left\langle \left| G(\omega) \sum_j e^{-i\omega t_j} + \frac{C}{2i} \sum_{n=1}^N \left[B_n e^{-in\omega_0\phi_n} G(\omega - n\omega_0) \sum_j e^{-i(\omega - n\omega_0)t_j} \right] \right|^2 \right\rangle + \right. \\ \text{(c)} \quad & \left. + 4\pi AT \text{sinc}\left(\frac{T}{2}\omega\right) \mathbf{Re} \left[G(\omega) < \sum_j e^{-i\omega t_j} > \right] + \right. \\ \text{(d)} \quad & \left. + \pi TC \sum_{n=1}^N B_n^2 \cos(n\omega_0\phi_n) \text{sinc}\left[\frac{T}{2}(\omega - n\omega_0)\right] \mathbf{Re} \left[e^{-in\omega_0\phi_n} G(\omega - n\omega_0) < \sum_j e^{-i(\omega - n\omega_0)t_j} > \right] + \right. \\ \text{(e)} \quad & \left. + \pi TC \sum_{n=1}^N B_n^2 \sin(n\omega_0\phi_n) \text{sinc}\left[\frac{T}{2}(\omega - n\omega_0)\right] \mathbf{Im} \left[e^{-in\omega_0\phi_n} G(\omega - n\omega_0) < \sum_j e^{-i(\omega - n\omega_0)t_j} > \right] \right\} . \end{aligned} \tag{A1}$$

Note that the cross products in term *b* cannot be neglected because of the considerable width of $G(\omega)$. However it can be shown that these cross products cancel each other exactly over the ensemble average. Term A1*b* becomes

$$4\pi^2 \left\{ |G(\omega)|^2 < \left| \sum_j e^{-i\omega t_j} \right|^2 > + \frac{C^2}{4} \sum_{n=1}^N \left[B_n^2 |G(\omega - n\omega_0)|^2 < \left| \sum_j e^{-i(\omega - n\omega_0)t_j} \right|^2 > \right] \right\} .$$

In order to calculate $< \left| \sum_j e^{-i\alpha t_j} \right|^2 >$, we separate real and imaginary parts of the sum and work out the ensemble average separately. We obtain

$$< \left| \sum_j e^{-i\alpha t_j} \right|^2 > = N + (N^2 - N) (< \cos \alpha t_j >^2 + < \sin \alpha t_j >^2) .$$

Note that, unlike the case of a random walk, the second terms become very large close to the resonance condition $\alpha = 0$ (i.e. $\omega = n\omega_0$ in Eq. A1). If the mean over the ensemble is

equal to the mean over time (i.e. the system is ergodic), we have

$$\langle f \rangle = \bar{f} = \frac{1}{T} \int_{-\frac{T}{2}}^{\frac{T}{2}} f(t) dt \quad ,$$

and

$$\langle \left| \sum_j e^{-i\alpha\theta_j} \right|^2 \rangle = N + (N^2 - N) \text{sinc}^2\left(\frac{\alpha T}{2}\right) \quad .$$

Term A1*b* therefore becomes:

$$\begin{aligned} & 4\pi^2 T\nu \left[|G(\omega)|^2 + \frac{C^2}{4} \sum_{n=1}^N B_n^2 |G(\omega - n\omega_0)|^2 \right] + \\ & \pi^2 C^2 (T^2 \nu^2 - T\nu) \sum_{n=1}^N B_n^2 \text{sinc}^2\left(\frac{(\omega - n\omega_0)T}{2}\right) |G(\omega - n\omega_0)|^2 \quad . \end{aligned}$$

Term A1*c* represents the contribution of the shot average to the zero frequency power, while terms A1*d* and A1*e* are simplified in a manner similar to A1*b*. We finally obtain Eq. 5.

REFERENCES

- Abramowicz, M., Bao, G., Lanza, A. & Zhang, X. H. 1991, *A&A*, 245, 454
- Angelini, L. 1989 in Proc. 23rd ESLAB Symp. on Two Topics in X-Ray Astronomy Eds. J. Hunt & B. Battrick (ESA SP-296, Noordwijk, NL), p.81
- Angelini, L., Stella, L. & Parmar, A.N. 1989, *ApJ* 346, 906
- Belloni, T. & Hasinger, G. 1990a, *A&A* 230, 103
- Belloni, T. & Hasinger, G. 1990b, *A&A* 227, L33
- Burderi, L., Robba, N. R. & Cusumano, G. 1993, *Adv. Sp. Sc.* 13, 291
- Elsner, R. F., Shibazaki, N. & Weisskopf, M. C. 1987 *ApJ* 320, 527
- Finger, M. H., Wilson, R. B. & Harmon, B. A. 1996, *ApJ*, 459, 288
- Hoshino, M. & Takeshima, T. 1993, *ApJ*, 411, L79
- Israel, G. L. & Stella, L., 1996, *ApJ*, *in press*
- Makishima, K. 1988 in *Physics of Neutron Stars and Black Holes*, Ed. Y. Tanaka (Universal Academy Press, Tokyo), p.175
- Makishima, K. et al. 1990, *PASJ* 42, 295
- Nagase, F. 1989 in Proc. 23rd ESLAB Symp. on Two Topics in X-Ray Astronomy Eds. J. Hunt & B. Battrick (ESA SP-296, Noordwijk, NL), p. 45
- Parmar, A.N., White, N.E., Stella, L., Izzo, C. & Ferri, P. 1989 *ApJ* 338, 359
- Shibazaki, N. & Lamb, F.K. 1987 *ApJ* 318, 767.
- Shinoda, K., Kii, T., Mitsuda, K., Nagase, F., Tanaka, Y., Makishima, K., & Shibazaki, N. 1990, *PASJ* 42, L27
- Soong, Y. & Swank, J. H. 1989 in Proc. 23rd ESLAB Symp. on Two Topics in X-Ray Astronomy Eds. J. Hunt & B. Battrick (ESA SP-296, Noordwijk, NL), p. 617
- Stella, L., White, N. E., Davelaar, J., Parmar, A.N., Blisset, R.J. & van der Klis, M. 1985, *ApJL* 288, L45.
- Sutherland, P.G., Weisskopf, M.C. & Kahn, S.M. 1978 *ApJ* 219, 1029

- Tagliaferri, G. & Stella, L. 1993, Mem. Soc. As. It. 64, 1075
- Tagliaferri, G. & Stella, L. 1994, Proc. ESO-OAT Workshop n.50 *Handling and Archiving Data from Ground-Based Telescopes*, Ed. M. Albrecht & F. Pasian (ESO, Garching), P.203
- Takeshima, T. 1992, PhD thesis, University of Tokyo
- Tanaka, Y. et al. 1983, IAU Circ. 3891
- Tennant, A. F. 1991 NASA Technical Mem. 4301 (NASA, Washington)
- Terrell, N. J. 1972 ApJ 174, L35
- van der Klis, M. 1989 in *Timing Neutron Stars*, Eds. H. Ögelman & E. P. J. van den Heuvel, NATO ASI Series C 262 (Kluwer, Dordrecht), p.27
- van der Klis, M. 1995, in *X-ray Binaries*, Eds. W. H. G. Lewin, J. van Paradijs & E. P. J. van den Heuvel (Cambridge University Press), p.252
- Weisskopf, M. C., Kahn, S. M. & Sutherland P.G. 1975, ApJ 199, L147
- White, N. E. & Peacock, A. 1988, Mem. Soc. As. It. 59, 7
- White, N. E. et al. 1995a in *Information and On-Line Data in Astronomy*, Ed. D. Egret & M. Albrecht (Kluwer, Dordrecht), p.139
- White, N.E., Nagase, F. & Parmar, A.N. 1995b, in *X-ray Binaries*, Eds. W. H. G. Lewin, J. van Paradijs & E. P. J. van den Heuvel (Cambridge University Press), p.1

Table 1: EXOSAT ME Observations

Name	Time (yy.ddd)	Seq.	Exposure (s)	Count Rate (cts/s)	^a N_{int}	^b T_{int} (s)	Δt (s)
Vela X-1	85.044	1402	37341	73.2	7	5120	5
4U1145-62	85.001	1324	34000	42.0	13	12400	10
	85.002	1326	21220	35.1			
	85.004	1329	24070	35.0			
	85.005	1332	23570	34.8			
	85.008	1339	25660	21.1			
Cen X-3	85.193	1697	40685	315.1	11	2048	0.5

^a Number of intervals used to calculate the average power spectrum.

^b Duration of each interval.

Table 2: Results from step *iii* fits.

	Vela X-1	4U1145-62	Cen X-3
R	3.2 ± 0.2	1.6 ± 0.2	< 0.66
CB_1	$0.61^{+0.13}_{-0.11}$	$0.79^{+0.17}_{-0.17}$	< 0.37
CB_2	$0.63^{+0.10}_{-0.09}$	$0.29^{+0.09}_{-0.08}$	< 0.23
CB_3	$0.10^{+0.03}_{-0.03}$	$0.07^{+0.03}_{-0.02}$	< 0.06
CB_4	$0.41^{+0.07}_{-0.06}$	$0.25^{+0.07}_{-0.06}$	-
CB_5	$0.44^{+0.07}_{-0.06}$	$0.17^{+0.05}_{-0.05}$	-
CB_6	$0.22^{+0.04}_{-0.03}$	-	-
CB_7	$0.26^{+0.05}_{-0.04}$	-	-
CB_8	$0.14^{+0.03}_{-0.03}$	-	-
CB_9	$0.10^{+0.03}_{-0.03}$	-	-
CB_{10}	$0.11^{+0.03}_{-0.02}$	-	-
CB_{11}	$0.14^{+0.03}_{-0.02}$	-	-

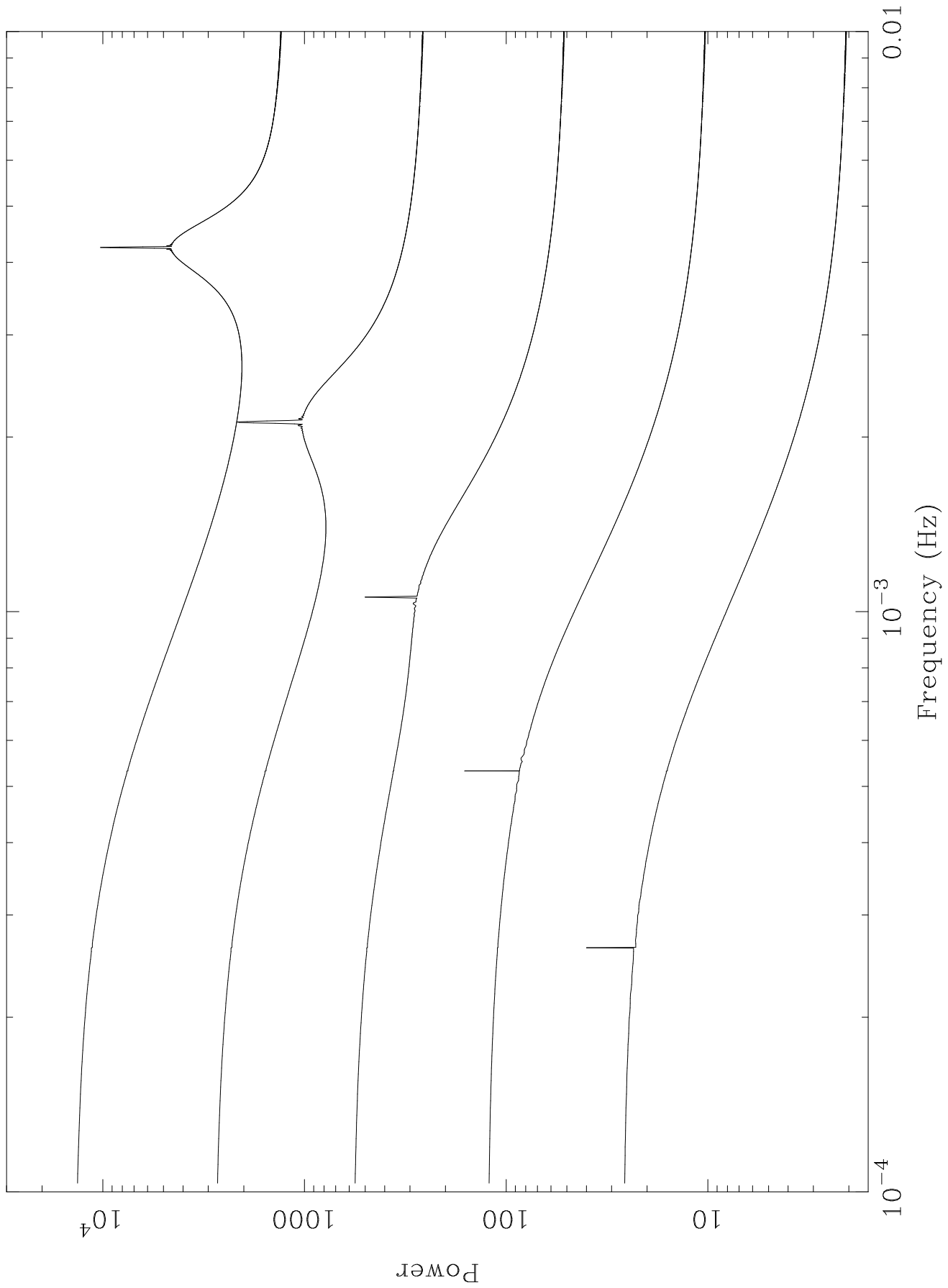
Fig. 1.— Model power spectra (cf. Eq. (5)) for shots with an exponential envelope function of decay time $\tau = 300$ s. The shots are 50% modulated with a sinusoidal signal. Different curves corresponds to different values of the period P ; from the top to the bottom this is 236, 471, 942, 1885 and 3770 s. The adopted light curve duration and binning time were 512000 s and 5 s, respectively. It is apparent that the width of broad wings below the sharp peak increases as P decreases.

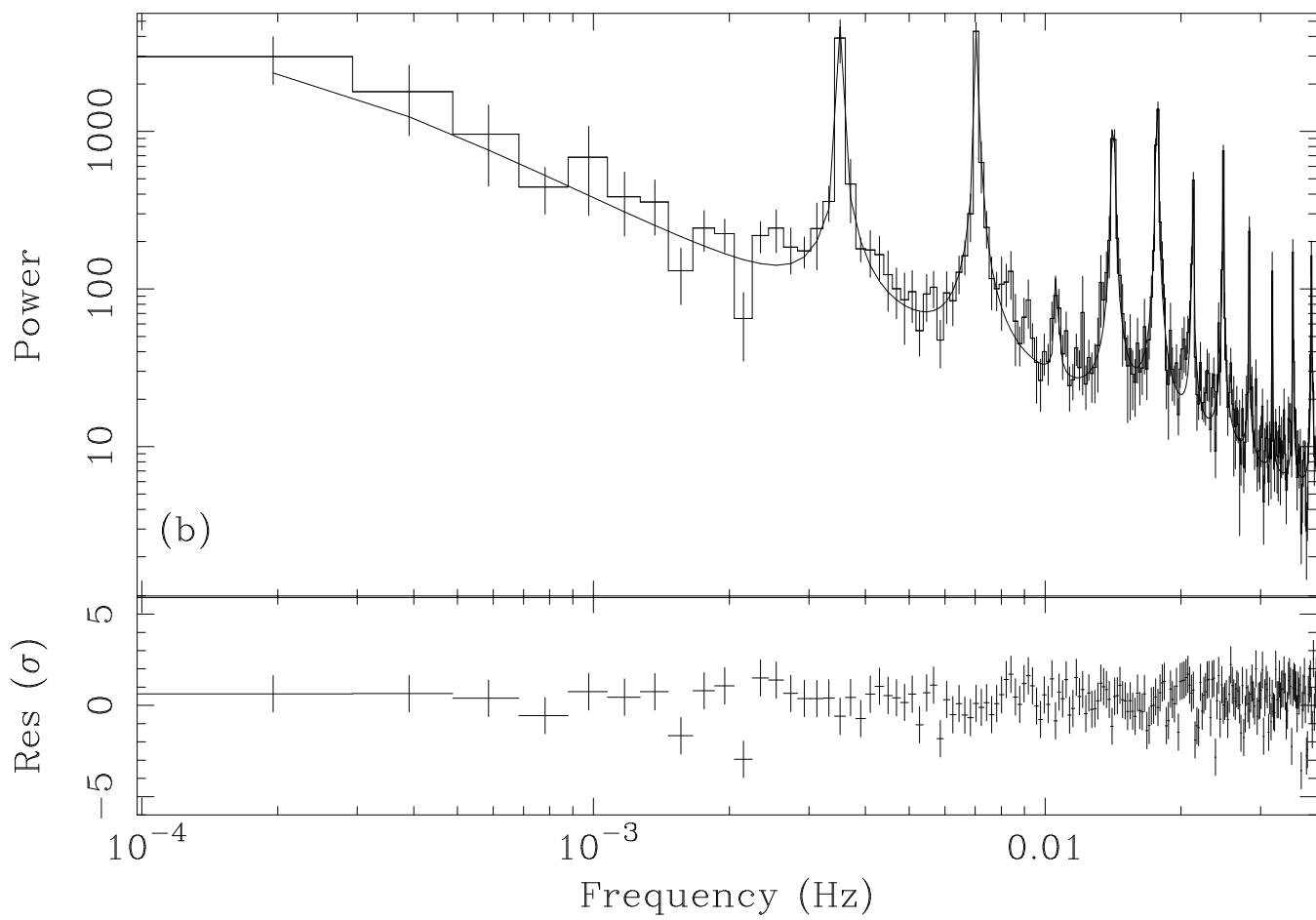
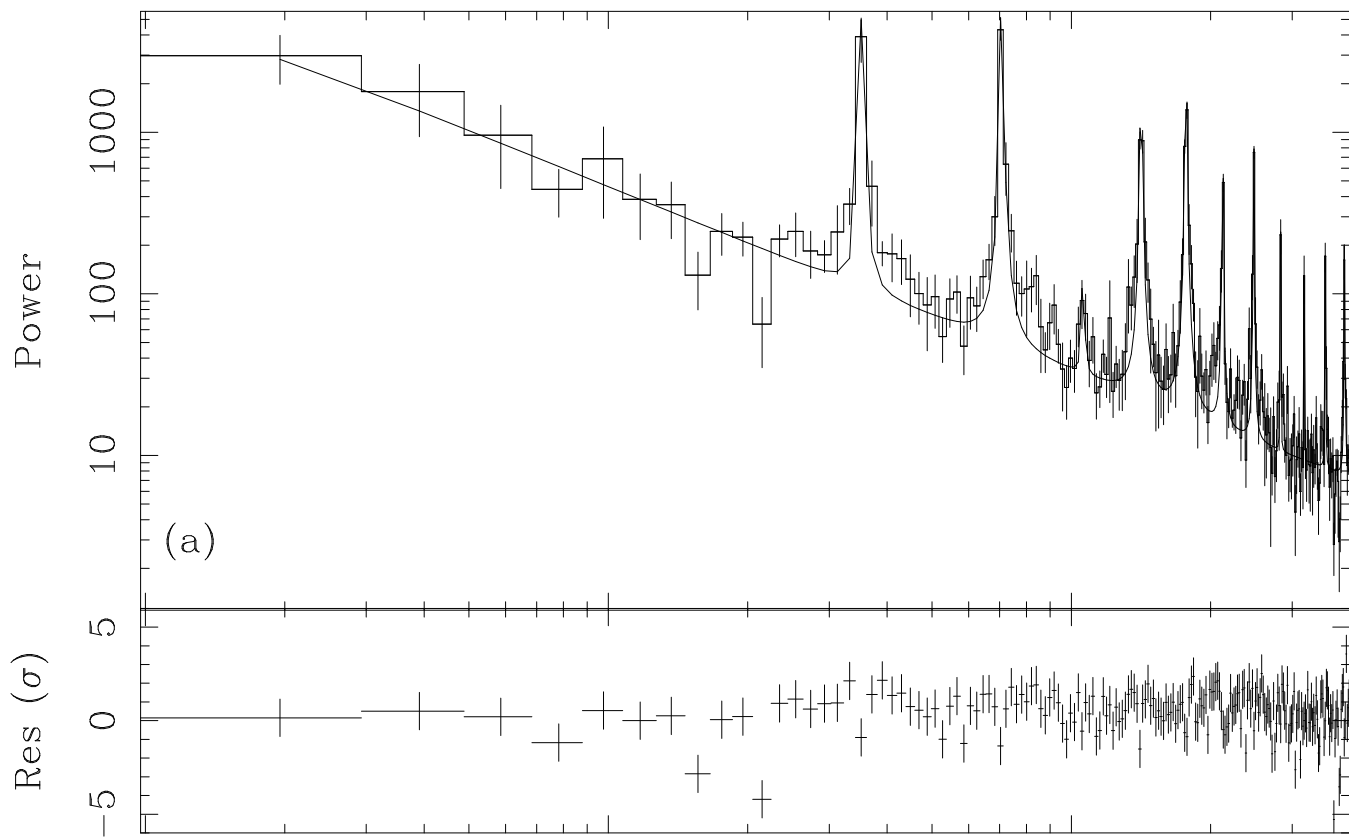
Fig. 2.— Average power spectrum obtained from the EXOSAT light curves of Vela X-1, together with the best fit models obtained in the case of non-modulated shots (step *i*, panel *a*) and modulated shots (step *iii*, panel *b*). The lower part of each panel shows the corresponding residuals.

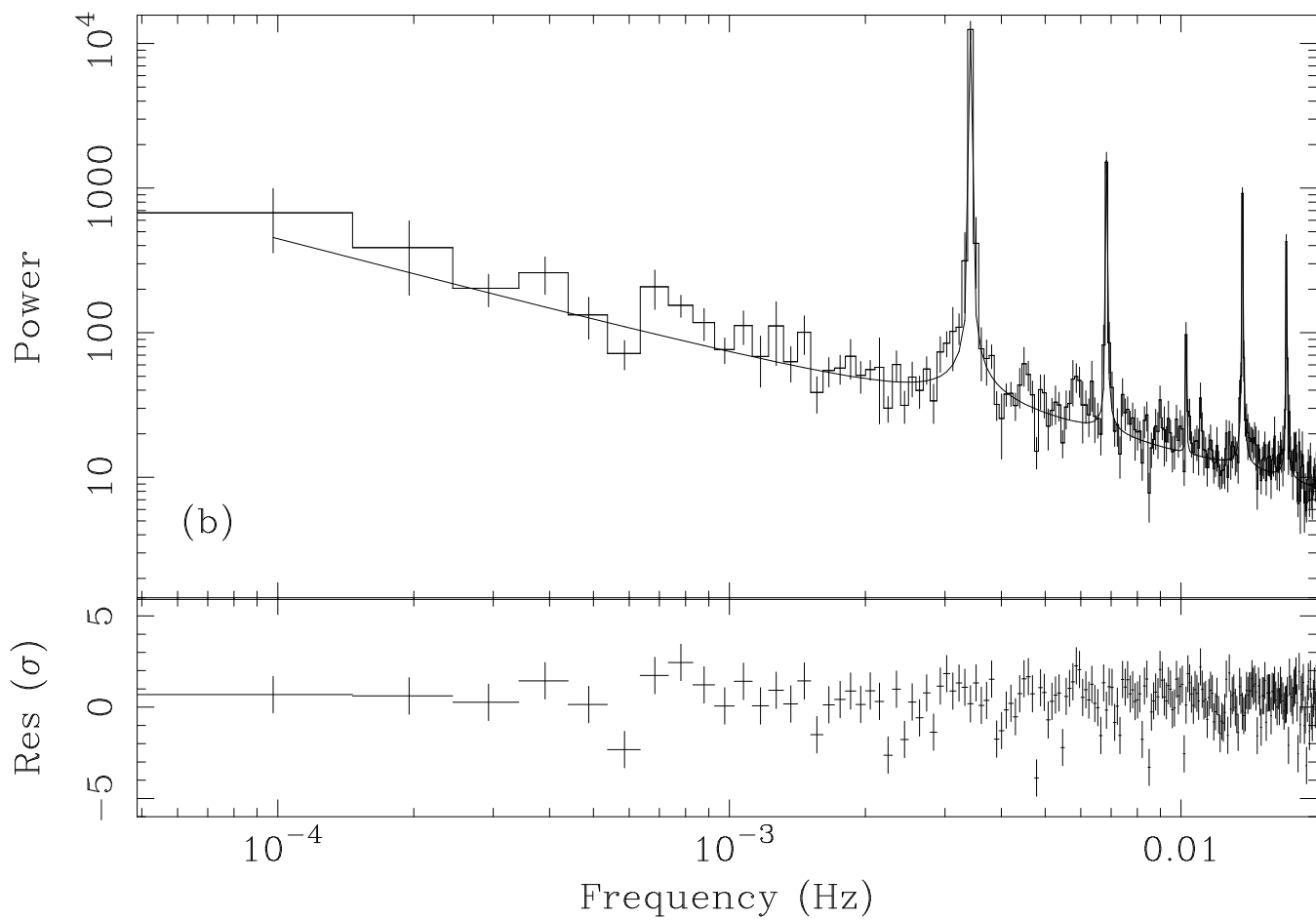
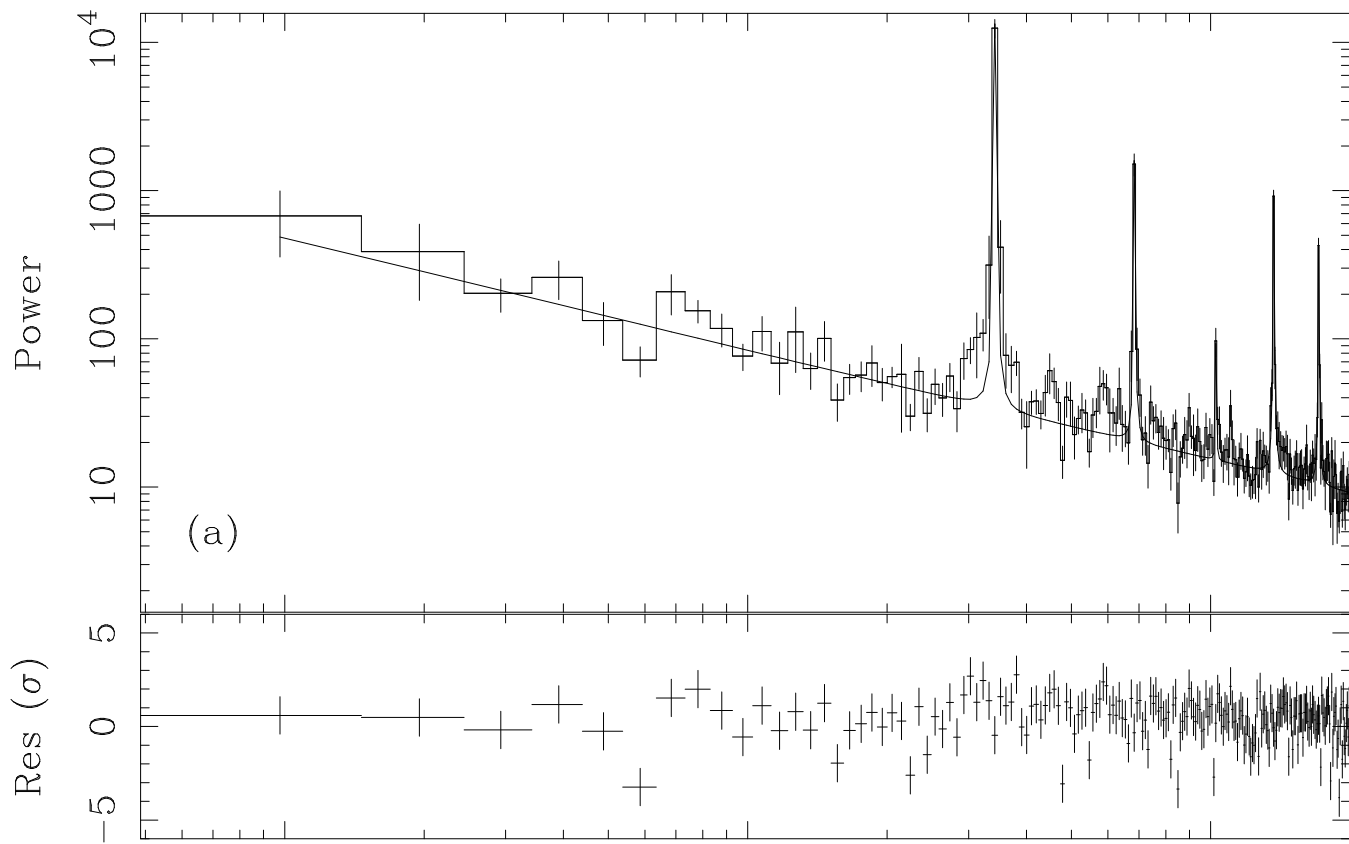
Fig. 3.— Average power spectrum obtained from the EXOSAT light curves of 4U 1145-62, together with the best fit models obtained in the case of non-modulated shots (step *i*, panel *a*) and modulated shots (step *iii*, panel *b*). The lower part of each panel shows the corresponding residuals.

Fig. 4.— Average power spectrum obtained from the EXOSAT light curves of Cen X-3, together with the best fit models obtained in the case of non-modulated shots (step *i*) and modulated shots (step *iii*). In this case the two fits are virtually identical. The lower part of the figure shows the corresponding residuals.

Fig. 5.— Comparison between the best fit to the average spectrum of Vela X-1 obtained with model of Takeshima (panel *a*) and the modulated shot model (step *iii*, panel *b*). The contribution from the three components of each model is also plotted. The lower part of each panel shows the corresponding residuals.







CEN X-3 EXOSAT ME 4-9 keV

